

Molecular Motion and Molecular Interaction in the Nematic and Isotropic Phases of a Liquid Crystal Compound

BY MYRON EVANS AND (IN PART) MANSEL DAVIES AND IAN LARKIN

University College of Wales, Edward Davies Chemical Laboratories,
Aberystwyth SY23 1NE

Received 30th August, 1972

The far infra-red absorption ($6\text{--}200\text{ cm}^{-1}$) of a typical liquid crystal compound [*N*-(*p*-methoxybenzylidene)-*p*-*n*-butylaniline: MBBA] has been studied over the nematic range (295–320 K) and beyond (up to 358 K); ten per cent concentrations in cyclo-octane (297 to 338 K); fifty per cent concentrations in *n*-octane (297 to 334 K); down to four per cent concentrations in benzene (296 K); and in d.c. fields up to 9 kV cm^{-1} .

The far infra-red is dominated by a strong feature centred near 130 cm^{-1} , both sharper and of higher frequency than the Poley absorptions characteristic of most isotropic polar liquids to which the MBBA tends on dilution with increasing temperature. Qualitative and quantitative aspects show the 130 cm^{-1} absorption to arise from the librational mode about the long axis of the MBBA molecules. The contour of the absorption (including that of the microwave region) is fitted in terms of both the Brot and Wyllie molecular-dynamic models with closely comparable apparent energy-well depths (16 to 19 kJ mol^{-1}). This appraisal is supported by *a priori* calculations of the form and depth of the energy wells in terms of the parameters established for phenyl-ring interactions in the Rae–Mason evaluations of the lattice energy of benzene.

Recent studies^{1–6} have established that the microwave and far infra-red absorptions (from 0.1 to 170 cm^{-1}) of rigid polar molecules in the liquid state are compounded of two principal broad band components: (i) the co-operative reorientation of the molecules in the applied field, leading to the Debye relaxation mode absorption (centred at *ca.* 1 cm^{-1}); (ii) the higher frequency absorption (*ca.* 70 cm^{-1}) due to the librational oscillation of each polar molecule within the cage formed by its neighbours. The latter absorption is related to the gas phase rotational mode absorption^{7–9} but its frequency is controlled by the depth and contour of the instantaneous energy wells in which the molecules execute their librational oscillations. Various models have been developed to represent the spectroscopic consequences of the simultaneous presence of these two not entirely distinct processes (see references in the Discussion section). Recent evaluations¹⁰ of the models due to Brot and Wyllie have shown that, with a minimum of arbitrary detail, the absorptions observed for some rigid polar molecules, including benzene derivatives and, in particular, a number of rotator phase compounds, can be adequately fitted on the basis of local intermolecular energy wells of quite acceptable values.

The nematic phase of a liquid crystal offers a particularly interesting situation in which to test these models further. A liquid crystal is characterised by the tendency of molecules to lie with their long axes parallel even when they are separated by large distances. This conclusion is associated with the essentially normal permittivity of the nematic liquid in relation to the effective resultant electric moment of the monomer molecules of the liquid crystal. [The permittivity and other (including microwave) data for the system described will be reported shortly.¹¹] The liquid crystal specie

reported in this paper is *N*-(*p*-methoxybenzylidene)-*p*-*n*-butylaniline: MBBA, whose melting point is 295 K and transition point to the isotropic liquid 320 K.

EXPERIMENTAL

The spectra were obtained^{1, 12} with a standard Grubb Parsons/N.P.L. "cube" interferometric spectrometer, of normal scanning range 10-200 cm⁻¹. A spectrum of nematic MBBA at 296±1 K was run at the N.P.L., Teddington (using a Beckman lamellar-grating interferometer with a helium cooled Putley detector) from 6 to 45 cm⁻¹. For pure MBBA, best discrimination on $\alpha(\bar{\nu})$ was given by a sample path length difference of 0.16 mm. Direct comparison of $\alpha(\bar{\nu})$ with and without the presence of an applied d.c. field was obtained using a variety of fixed path-length cells especially constructed for this purpose, using wire (0.075 mm o.d.) electrodes between two spacers. No attempt was made to obtain a uniformly oriented sample of the mesophase by pretreatment of the surfaces of the cell.

The spectra for samples above room temperature were taken in an electrically heated variable path-length cell, the fluctuations in temperature (read from a calibrated thermocouple) being typically ±2 K.

Judged by the sharpness of the nematic-isotropic transition at 320 K, the MBBA sample used (from Eastmann-Kodak Ltd.) was of an acceptable purity. It was kept dry by standing over type 3A zeolite, when not in use, under nitrogen at 273 K. To check on decomposition several interferograms were run (for up to 3 h) in the isotropic phase at 358 K, then the cell was cooled and several further spectra were recorded at 296 K. The latter $\alpha(\bar{\nu})$ values agreed within ±5% with those obtained from fresh, pure, unheated samples. Thin layer chromatographs could detect no difference between these latter and samples held at 358 K for 3 h. Solutions were made up by weight in pure, dry solvents.

The mean $\alpha(\bar{\nu})$ values presented have an uncertainty of ±5% or less except at $\bar{\nu} > 170$ cm⁻¹, due to beam divider characteristics, and, occasionally at 130±5 cm⁻¹ owing to the intensity of the peak absorptions there. All accepted spectra were the weighted means of at least three sample runs usually at each of two thicknesses, ratioed against three background runs. Evaluations of the integrated intensity $\int_{\text{band}} \alpha(\bar{\nu}) d\bar{\nu}$ involves extrapolation of the observed $\alpha(\bar{\nu})$ at both high and low values. With the aid of microwave measurements the extrapolation to $\bar{\nu} = 0$ leaves relatively little uncertainty, but at $\bar{\nu} > 170$ cm⁻¹ the absorption centred near 130 cm⁻¹ is overlapped by a neighbouring feature: the contribution of the latter has been estimated to result in an uncertainty of ±10% in the integrated intensity being determined.

RESULTS

The measurements are summarized in table 1, and fig. 1, 2 and 3 are a small selection of the spectra (all having α values usually defined within ±5%) on which the data are based. The changes seen in the field of 7 kV cm⁻¹ were also found at proportional levels for 2.5 and 9.1 kV cm⁻¹.

The nematic phase absorption at 130 cm⁻¹ has a flattened peak and considerable intensity, far beyond that anticipated for a difference tone or an intra-molecular torsional mode in the MBBA molecule: neither the half width nor the intensity are plausibly associated with the latter mode. But the Poley absorption is of this half-width and intensity ($\Delta\bar{\nu}(\frac{1}{2}) = 80$ cm⁻¹; $\alpha_{\text{max}} = 85$ neper cm⁻¹) in typical polar liquids (e.g. for benzonitrile $\Delta\bar{\nu}(\frac{1}{2}) = 70$ cm⁻¹; $\alpha_{\text{max}} = 95$ neper cm⁻¹); and this absorption must be expected above $\bar{\nu} = 50$ cm⁻¹ in MBBA. That it is centred near 130 cm⁻¹ is a consequence of the deeper and narrower energy wells in which the lath-like molecules librate. X-ray evidence¹⁴ implies that around each molecule there is approximately a hexagonal array of parallel molecules.

As model calculations (see later) confirm, this environment provides rather sharply defined energy wells with respect to angular displacement even about the long axis, and a correspondingly high librational frequency.

TABLE I.—QUANTITATIVE EXPERIMENTAL OBSERVATIONS

temp./K (± 2)	phase	solvent	w/w (%)	field/ kV cm ⁻¹	$\bar{\nu}(\text{max})/$ cm ⁻¹	$\alpha(\text{max})/$ neper cm ⁻¹	half width/ cm ⁻¹
296	nematic	—	—	0	130 \pm 5	85	80
341	isotropic	—	—	0	123 \pm 3	72	80
359	isotropic	—	—	0	123 \pm 3	63	75
297	isotropic	cyclo-octane	10.2	0	133 \pm 3	8.0	60
324	isotropic	cyclo-octane	10.2	0	130 \pm 2	5.2	80
338	isotropic	cyclo-octane	10.2	0	130 \pm 2	4.0	130
296	isotropic	n-octane	50.2	0	130 \pm 2	30	65
334	isotropic	n-octane	50.2	0	125 \pm 2	23	100
296	isotropic	benzene	67.4	0	128 \pm 2	52	60
296	isotropic	benzene	25.2	0	128 \pm 2	15	60
296	isotropic	benzene	10.7	0	128 \pm 2	8.5	60
296	isotropic	benzene	4.1	0	128 \pm 2	3.3	60
296	nematic	—	—	7	133 \pm 2	83	75
296	nematic*	—	—	0	130 \pm 2	100	85
283	solid	—	—	0	{ 130 \pm 3 97 \pm 2	79	80
						79	(overall)

* measurement prior to field measurement.

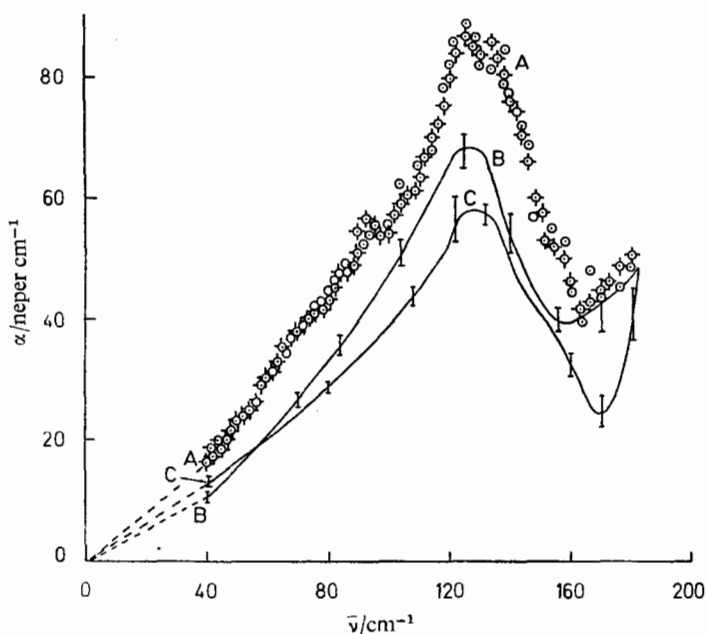


FIG. 1.—(A) Spectrum of nematic MBBA at 296 ± 0.5 K \diamond — mean of three interferograms at a thick path length ratioed to the mean of three interferograms at a thin path length. \circ An individual thick path length interferogram ratioed to the latter mean. Path length difference = 0.140 mm: with polythene windows. (B) Spectrum of isotropic MBBA at 341 K. For clarity, the experimental data (which are of the same form as in (A)) are represented by a curve, error bars at selected points representing the difference between the *greatest* and *least* values of α obtained at a given $\bar{\nu}$. Path length difference is 0.186 mm: with TPX windows. (C) Spectrum of isotropic MBBA at 359 K, presented as in (B). Path length difference = 0.150 mm; with TPX windows.

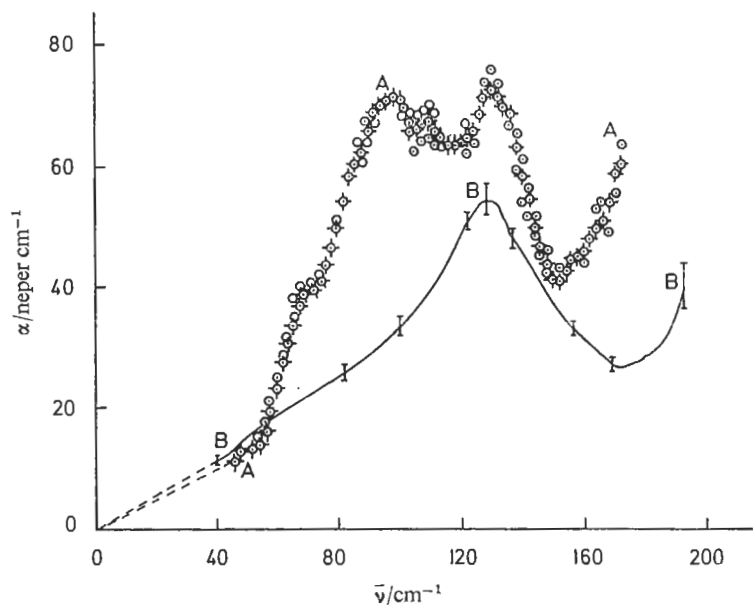


FIG. 2.—(A) Spectrum of crystalline MBBA at 283 ± 1 K, presented as in fig. 1A except that ratios were on a sample/background basis as a fixed path-length cell was used. Thickness of sample = 0.16 mm; with polythene windows and Teflon spacers. (B) Spectrum of a 67.3 w/w per cent solution of MBBA in benzene at 296 ± 0.5 K, corrected for solvent absorption. Path length difference = 0.25 mm with polythene windows.

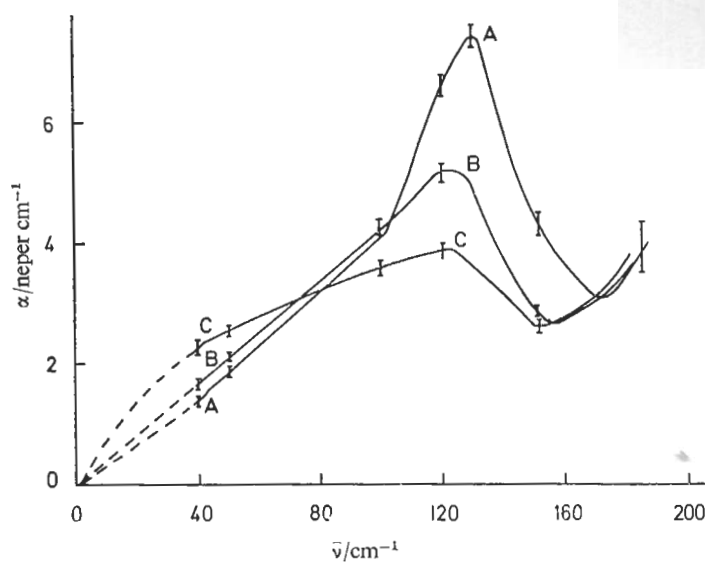


FIG. 3.—(A) Spectrum of a 10.2 w/w per cent solution of MBBA in cyclo-octane (corrected as in fig. 2 for solvent absorption), presented as in fig. 1B, at 297 ± 0.5 K. Path length difference = 1.50 mm with TPX windows. (B) As in (A), but at 324 ± 1 K, path length difference = 1.75 mm. (C) As in (A), but at 338 ± 1 K, path length difference = 1.50 mm.

Measurements on both instruments agree that the absorption is a rising continuum from 6 cm^{-1} to the peak at $130 \pm 5 \text{ cm}^{-1}$. Moreover, a resolution of 2 cm^{-1} on the lamellar grating interferometer revealed no new superimposed detail on this main band, the agreement in $\alpha(\bar{\nu})$ values being excellent in the overlap region of $40\text{--}45 \text{ cm}^{-1}$. Thus the only region left unobserved for nematic MBBA at $296 \pm 1 \text{ K}$ is the 1.25 cm^{-1} to 6 cm^{-1} region where no startling deviations from the continuum are expected, or indeed, are suggested by the present data.

Further features consistent with the assignment of the 130 cm^{-1} absorption to a Poley absorption are the absence of any evidence for this centre below 100 cm^{-1} and the improbability of it occurring above 170 cm^{-1} . Heating and/or dilution provides displacement in $\bar{\nu}(\text{max})$ as expected, certainly larger than would occur for an intramolecular mode, but perhaps less than might be anticipated for the nematic \rightarrow isotropic phase change until it is recalled that close-range order scarcely differs between these phases as is emphasized by de Vries.¹⁴ The present spectra (only a few are reproduced in this paper) together with the dielectric data for pure MBBA and its solutions, are consistent with only slight change in this near-neighbour interaction even on markedly changing the temperature and diluting. Only by taking a 10 % solution in cyclo-octane to 18 K above the transition temperature (which is 320 K) was a quite extensive change in the absorption produced, the change itself being conclusive evidence that its origin was not that of an intramolecular mode. Finally, application of a d.c. field produced small but real changes which are presumably caused by a change from a state in which the director is disorganised to one in which it is parallel to the electric field, in other words the absorption depends on the uniformity in the alignment of the director. None of these treatments produced noticeable shifts in the adjacent absorption (180 to 200 cm^{-1}) which is taken to be of proper-mode origin.

Experimental results and theoretical appraisal agree that the Poley absorption is essentially part of the molecular rotational mode, i.e. it is a high frequency adjunct to the microwave (Debye) relaxational absorption. Accordingly, the total intensity from $0\text{--}200 \text{ cm}^{-1}$ must be accepted as the molecularly relevant unit for discussion. Even so, there are two alternative versions of the integrated intensity. The first leads to the optical absorption cross-sectional area

$$a_1 = A_1/N = (1/N) \int_{\text{band}} \alpha(\bar{\nu}) d\bar{\nu} \quad (2.1)$$

where N is the MBBA molecular number density (in molecules cm^{-3}), the observed α values being corrected for the influence of the refractive index by means of the Polo-Wilson factor (see table 2). In addition, an electric permittivity dispersion amplitude can be determined from A_2 and the Kramers-Krönig relation:

$$A_2 = \int_{\text{band}} \epsilon''(\bar{\nu}) d(\log_e \bar{\nu}) = (\pi/2)(\epsilon_0 - n_{ir}^2) \quad (2.2)$$

Here $(\epsilon_0 - n_{ir}^2)$ is the dipole dispersion amplitude and

$$\epsilon''(\bar{\nu}) = \frac{n_{ir}\alpha(\bar{\nu})}{2\pi\bar{\nu}} \quad (2.3)$$

A_1 and A_2 will not lead to the same values of the effective molecular dipole moments for several reasons: an immediately relevant one is that A_1 will (in practice) include any collisionally induced component^{7,13,15,17,18} whereas A_2 will give (within the approximation allowed by internal field factors) a measure of the permanent (relaxing) dipole moment. In table 2 the a_1 (corrected) values show a maximum in

the pure nematic phase values and decrease generally with rising temperature and dilution. [The cyclo-octane 10.2 per cent solution at 297 K is anomalous, and should *perhaps* be regarded as erroneous.] The first conclusion from the a_1 values is that their first-order constancy for different concentrations and temperatures shows

TABLE 2.—CALCULATION OF $(1/N) \int_{\text{band}} \alpha(\bar{\nu}) d\bar{\nu}$ FOR MBBA (NEMATIC AND ISOTROPIC) AND SOLUTIONS OF MBBA IN *n*-OCTANE AND CYCLO-OCTANE

solvent	per cent w/w MBBA	$10^{-20} \times$ number density of MBBA in solution/ molecule cm^{-3} (= N_{MBBA})	Polo- Wilson factor (= X)	$A_1/$ neper cm^{-2}	$10^{20} \times A_1/N_{\text{MBBA}}$ = a_1/cm	temp./K	A_2
cyclo-octane	10.2	1.96	0.92	650 ± 60	300 ± 50	297 ± 0.5	1.8 ± 0.2
cyclo-octane	10.2	1.96	0.92	510 ± 50	240 ± 40	324 ± 1	1.7 ± 0.2
cyclo-octane	10.2	1.96	0.92	480 ± 50	224 ± 40	338 ± 1	1.9 ± 0.2
<i>n</i> -octane	50.2	9.67	0.77	2700 ± 300	220 ± 35	297 ± 0.5	—
<i>n</i> -octane	50.2	9.67	0.77	2460 ± 250	190 ± 30	334 ± 2	—
pure MBBA (nematic)	100	24.5	0.70	8905 ± 900	250 ± 40	296 ± 2	3.6 ± 0.3
pure MBBA (isotropic)	100	$(19.5) \pm (?)$	(0.70)	6620 ± 700	240 ± 40	341 ± 2	3.5 ± 0.3
pure MBBA (isotropic)	100	$(17.6) \pm (?)$	(0.70)	5520 ± 550	220 ± 35	358 ± 2	—

the absorption throughout to be of a common origin. It is also clear that the observed increase in half-width and the shift to lower frequency of $\bar{\nu}(\text{max})$ as the temperature rises are consistent with the librational mode in the near-neighbour field. There are probably two features of the enhanced molecular order in the nematic phase which tend to maximise the observed a_1 values there. In passing from the random molecular orientational state (characteristic of the normal isotropic liquid) to one of higher order, part of the dipole relaxation tends to be transferred from the cooperative relaxation process in the microwave region to the librational mode of the far infra-red: in the limit of the normal crystalline state the (Debye) relaxational absorption is completely lost, its intensity being distributed among much higher frequency librational modes in the lattice. Owing to the relation between ϵ'' and α , a_1 will be increased by this transfer, as occurs in the observed values for MBBA on enhancement of the molecular "pseudo-lattice" order. This order is thus a feature contributing to the unusual intensity of the 130 cm^{-1} absorptions in the nematic phase.

Another contribution to a_1 will arise from the collisionally induced and other transient moments generated in condensed phases. Not only in non-dipolar liquids do such absorptions become obvious but for the markedly anisotropic nitrous oxide ($\text{N}=\text{N}=\text{O}$) molecule, the quadrupole-induced absorption in the liquid state exceeds in intensity that due to the (small) permanent moment. The collisionally induced absorptions could well become considerable for this highly polar and markedly polarizable MBBA molecule: the molecular features mentioned being significant contributors in the formation of the nematic phase.

DISCUSSION

The spectroscopic observations have been interpreted with two models which each envisage a central molecule instantaneously surrounded by a certain number of neighbours. This coordination number defines the angular aperture of the energy

wells in which the molecule librates; the contour of the supposed identical energy wells and their depth ($n kT$) providing parameters¹⁰ which have to be chosen to match the observed spectrum. The microwave absorptions (in low electric fields) of MBBA, which have been measured¹¹ recently both in the nematic and isotropic states, essentially define the absorption up to 10 cm^{-1} in terms of $(\epsilon_0 - \epsilon_\infty)$ and the effective (Debye) relaxation, and are introduced here for comparison with the theoretical results. The details of the microwave measurements and subsequent deduction of the τ_D values will be reported later.

The first model was developed by Brot^{20, 21} and extended by Larkin.¹⁰ The parameters shown in table 3 (and also table 4) follow the notation of ref. (10). The

TABLE 3.—BROT PARAMETERS AND COMPARISON WITH OBSERVATIONS FOR MBBA

temp./K	barrier height $V/\text{kJ mol}^{-1}$	$\tau_0(\text{obs.})/\text{ps}$	τ_r/ps	time of jump, τ_j/ps	$\xi/\text{deg.}$	$\omega_0(\text{obs.})/\text{cm}^{-1}$	$\omega_0(\text{calc.})/\text{cm}^{-1}$	narrowing factor
296 ± 2	16.(1)	250 ± 13	286	0.41	44	130 ± 5	124	0.29_6
341 ± 2	14.(3)	70 ± 3	65	0.42	44	123 ± 3	116	0.29_6
296 ± 2	18.(2)	250 ± 13	280	0.27	30	130 ± 5	124	0.46_3
341 ± 2	17.(1)	70 ± 3	170	0.42	30	123 ± 3	120	0.46_3

TABLE 4.—WYLLIE PARAMETERS AND COMPARISON WITH OBSERVATIONS FOR MBBA

temp./K	$V/\text{kJ mol}^{-1}$	$\tau_0(\text{obs.})/\text{ps}$	$\xi/2kT/\text{ps}$	Z	$\omega_0(\text{obs.})/\text{cm}^{-1}$	$\omega_0(\text{calc.})/\text{cm}^{-1}$	narrowing factor
296 ± 2	18.(9)	250 ± 13	296	6	130 ± 5	128	0.46_3
341 ± 2	15.(7)	70 ± 3	110	6	123 ± 3	116	0.46_3

moments of inertia needed in the calculation were estimated, with limiting uncertainty, by the method of Hirschfelder.²³ X-ray evidence¹⁴ suggests that the packing of nematogens is well ordered and that rotation, even about these long axes, will not be easy. An idealised hexagonal packing in the nematic phase,¹⁴ yields a calculated macroscopic density of:

$$\rho = M/(NlD^2 \cos 30^\circ) \quad (3.1)$$

(where M is the molecular weight, N is Avogadro's number, l the van der Waals distance between the hydrogens at the extremes of a stretched molecule, D the mean intermolecular distance) which is in a good agreement with observed densities for several nematogens. Therefore (3.1) was used to calculate a mean intermolecular distance D of 5.6 \AA , which when compared with the covalent van der Waals width of a benzene ring (6.7 \AA para H to H) supports the view that the only libration possible with a relatively small barrier to rotation would be that about the long axis of the molecule. A limiting uncertainty in the evaluation is that provided by the moment of inertia of the molecule about its long axis. For the purpose of the Hirschfelder calculation, the two configurations of fig. 6(e) were used, and the mean of the resulting values of the relevant I was $I = (470 \pm 30) \times 10^{-40} \text{ g cm}^2$.

For the rotator phase molecules¹⁰ (whose site models with the spherical-packing "coordination number" of twelve is well established, and for which experimental data are rather well defined) an acceptable fit to both τ_0 ($\approx \tau_r$) and ω_0 (the observed far infra-red librational peak position) can be obtained with the simple energy well contour of ref. (10). For MBBA and the Brot model a similar fit with observation is only possible if the energy well apertures are sharpened: the best simple fit requiring a sharpening to 0.30 of the original. There can be no great objection to this sharpening of the contour, since the original form is arbitrary, and chosen for the sake of simplicity.

With the molecular geometry given above, acceptable reproduction of the observed absorptions (see fig. 4 and 5) is achieved using a half angular aperture $\xi = 44$ or 30° . The value of $\xi = 44^\circ$ is obtained by an interaction potential calculation (see later) when the central molecule is rotated with its hexagonally arranged neighbours fixed—the repulsion being greatest at $\xi = 44^\circ$ for $D = 5.6 \text{ \AA}$. The value of $\xi = 30^\circ$ represents the other extreme (i.e. the position of maximum repulsion envisaged for

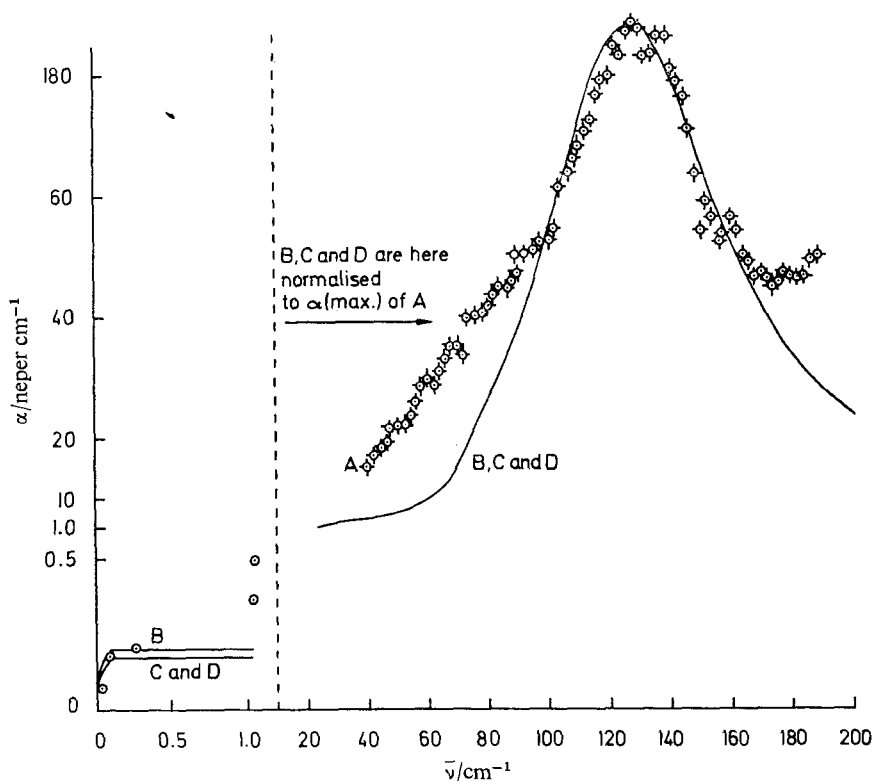


FIG. 4.—(A) \odot — Mean of eleven ratios (using different samples of MBBA) for nematic MBBA at 296 K, with various path length differences, and polythene and TPX windows. (B) Theoretical curve predicted by the Brot model at 296 K, with $\tau_r = 280 \text{ ps}$, $\omega_0 = 124 \text{ cm}^{-1}$, $V = 18 \text{ kJ mol}^{-1}$, a well narrowing factor of 0.463, and $\xi = 30^\circ$. The theoretical curve for $\tilde{\nu} \geq 10 \text{ cm}^{-1}$ is normalised to the $\alpha(\text{max})$ of the experimental values. The theoretical curve for $\tilde{\nu} < 10 \text{ cm}^{-1}$ is the absolute value obtained from the parameters used. (C) As for (B) with $\tau_r = 286 \text{ ps}$, $\omega_0 = 124 \text{ cm}^{-1}$, $V = 16 \text{ kJ mol}^{-1}$, a well narrowing factor of 0.296, and $\xi = 44^\circ$. Part of the curve is normalised as in (B). (D) Theoretical curve from the Wyllie model at 296 K, giving $\xi/2 kT = 296 \text{ ps}$, $\omega_0 = 128 \text{ cm}^{-1}$, $V = 19 \text{ kJ mol}^{-1}$, using a well narrowing factor of 0.463 and assuming 6 nearest neighbours. Part of the curve is normalised as in (B). (B), (C) and (D) are very similar for $\tilde{\nu} \geq 10 \text{ cm}^{-1}$ and are represented by a single curve. \odot Experimental microwave data.¹¹

the most favourably coordinated motion of all seven molecules). It must be emphasized that the barrier heights deduced can only be order of magnitude in precision, but the results (see table 3) clearly show that a considerable barrier to rotation about the long axis exists in the nematic and even in the isotropic phase.¹⁴ This must mean that the immediate environment of the central molecule in the two phases remains similar except for a small decrease in the apparent barrier height to libration. In view of this, and the fact that the barriers deduced¹⁰ for liquid phase "pseudo-spherical" molecules such as 2-methyl-2-nitropropane or 2-chloro-2-nitropropane

rotation is particularly easy, are of the order of 5.5 to 11.8 kJ mol⁻¹, then the prediction of the Maier-Saupe theory²⁷ of a barrier to rotation about the *short* axis kJ mol⁻¹ in MBBA is disturbingly small. It seems that any attempt to relax at the short axis will require cooperative motion, with a barrier height of about kJ mol⁻¹ as measured in the MHz region by Agarwal *et al.* in this laboratory.

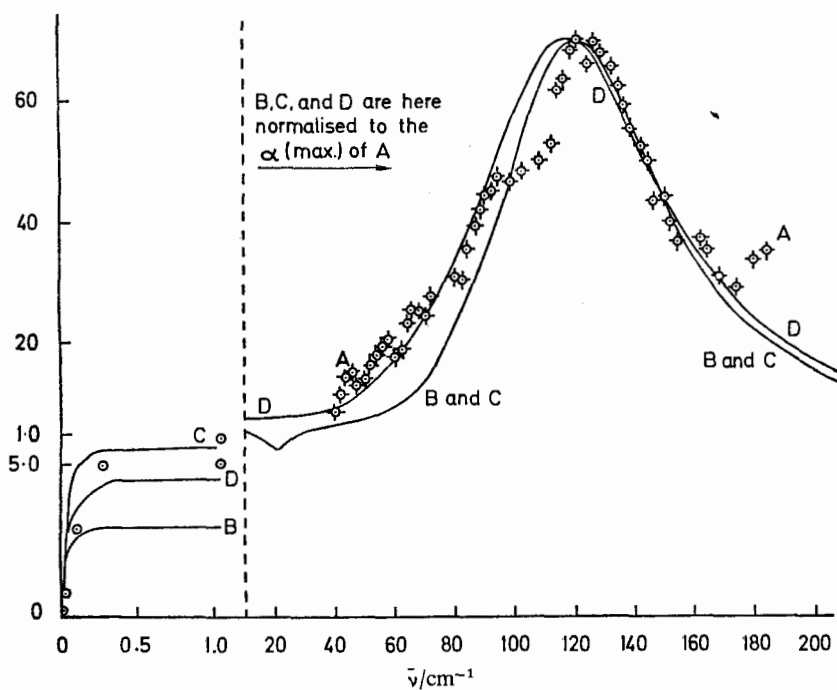


Fig. 5.—(A) \circ — Experimental mean values of α at 341 ± 2 K presented as in fig. 1A. Path length reference = 0.186 mm with TPX windows. (B) Theoretical curve from the Brot model at 341 K, with $\tau_r = 170$ ps, $\omega_0 = 116$ cm⁻¹, $V = 17$ kJ mol⁻¹, using a well narrowing factor of 0.463 and $\xi = 44^\circ$. Part of the curve is normalised as in fig. 9(B). (C) As for (B) with $\tau_r = 70$ ps, $\omega_0 = 116$ cm⁻¹, $V = 14$ kJ mol⁻¹, using a well narrowing factor of 0.296 and $\xi = 44^\circ$. Part of the curve is normalised as in fig. 9(B). (D) Theoretical curve from the Wyllie model at 341 K, giving $\zeta/2 kT = 110$ ps, $\omega_0 = 116$ cm⁻¹, $V = 16$ kJ mol⁻¹, using a well narrowing factor of 0.463 and assuming 6 nearest neighbours. Part of the curve is normalised as in fig. 9(B). (B) and (C) are very similar for $\bar{\nu} \geq 10$ cm⁻¹, and are represented by a single curve. \circ , Microwave data.¹¹

The absolute intensity observed for both the nematic and isotropic absorption is not correctly predicted by the Brot model. Contributions (discussed in the results section) to the observed absorption intensity which are neglected in our model can explain part of this excess. For example, the internal field correction of Polo and Vilson¹⁹ must be remembered, which reduces the measured integrated intensity by 10%. Also, the band whose absorption rises steeply above 170 cm⁻¹ provides a background which accentuates the apparent intensity of the librational mode. The large anisotropy of the polarisability of MBBA may be a contributing factor and there is going to be a spread in the shape and depth of the potential wells¹⁰ which will affect the α against $\bar{\nu}$ spectrum.

Our second model has been developed from the cooperative relaxation approach of Hill²⁴ and Wyllie²⁵ and extended by Larkin.¹⁰ Assuming an idealised arrangement of six nearest neighbours, as previously, then the parameters obtained from the

best fit to τ_0 and ω_0 and the observed contour are given in table 4, which again, notationally follows ref. (10). The barrier heights from both models agree to well within the significance that can be claimed, but again, the calculated absolute intensity is lower than the observed intensity. The agreement of experiment with the predictions of both models is satisfactory in the microwave region.

MODEL CALCULATIONS OF THE BARRIER HEIGHT

There is good agreement between the two models, giving values of the barrier height (14-19 kJ mol⁻¹) which are distinctly larger than those found in the rotator phase¹⁶ of polar molecules, but the values are essentially those fitting particular models. Therefore some independent estimate of V would be desirable. Such an estimate has been attempted on a simplified molecular force-field: the MBBA has been represented by two linked benzene residues, the van der Waals fields for the latter being already well established.

Rae and Mason²⁶ have shown how in benzene the intermolecular force field $U(r)$ is very well represented by terms of the form

$$U(r) = a \exp(-br) - c/r^6$$

to which contributions arise from the electron distributions in component (C-H) bonds, σ (C-C) bonds, and π (C-C) bonds. A recent X-ray study¹⁴ suggests that the packing in the nematic phase is only a loosened and irregular version of the

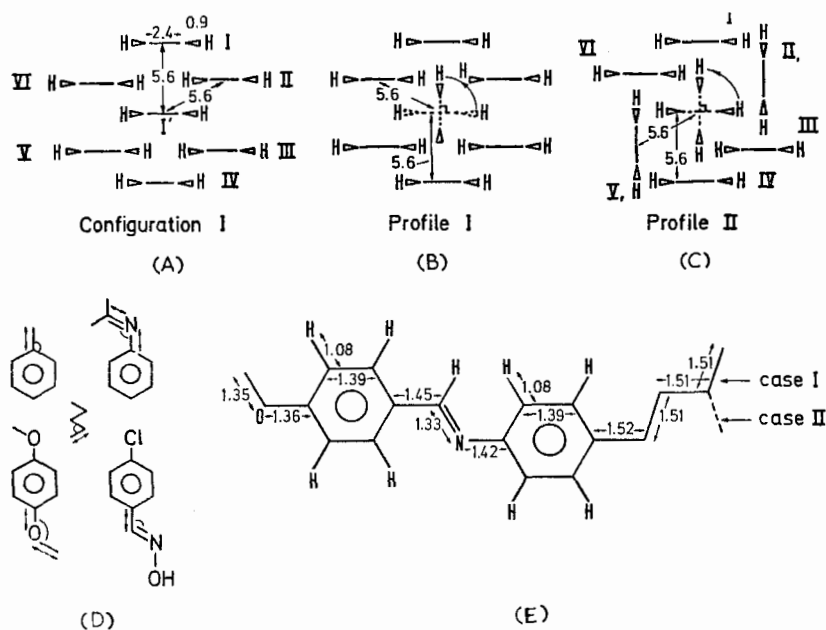


FIG. 6.—(A) Idealised hexagonal packing of MBBA molecules (approximated for the purpose of making a Rae-Mason calculation by two benzene rings), in the nematic phase. The long axis of each molecule is perpendicular to the plane of the paper. The two hydrogen atoms on each molecule are the *ortho* hydrogens of the phenyl ring. (B) The rotation of the central phenyl ring through 90°, keeping the outer six phenyl rings fixed, used as a basis for the first energy profile calculation. (C) The geometry, and rotation, used in the calculation of the second profile. (D) Representative bond lengths (arrowed) and angles (marked) in simple related molecules whose values have been assumed to apply in MBBA. (E) The two geometries used for the Hirschfelder calculation of the moment of inertia of MBBA (bond lengths in Å).

hexagonal close packing of the crystalline lattice. Each molecule is ideally surrounded by six nearest neighbours, which for present purposes, can be set at equal distances chosen so as to match the observed density of the nematic phase using the method of de Vries. This gives a centre to centre distance of the phenyl rings (see fig. 6(a)) of 5.6 Å. We now make the major assumption that the barrier to mutual rotation of the

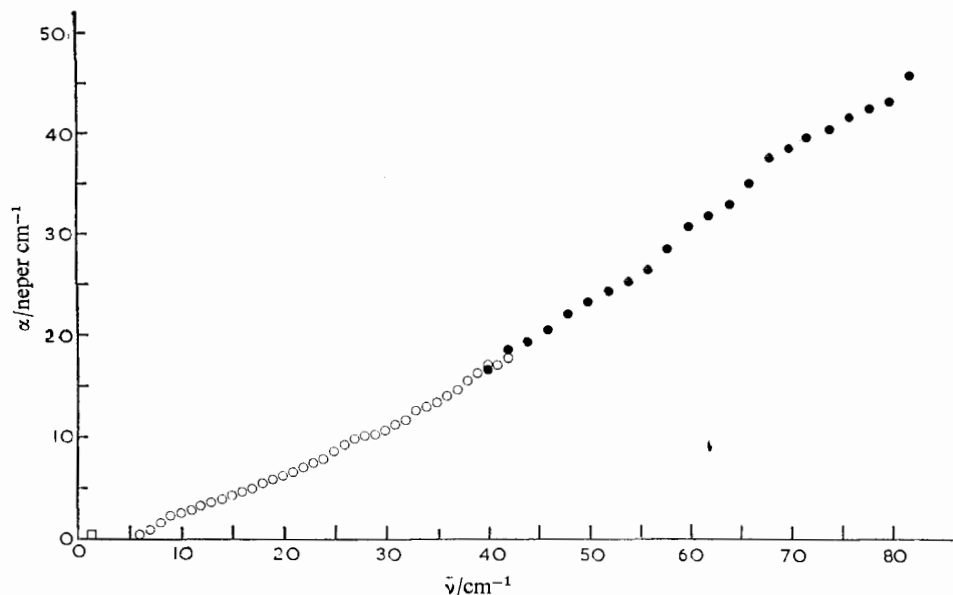


Fig. 7.—●, MBBA (nematic) at 296 ± 0.5 K, as in fig. 1A, taken with a resolution of 4 cm^{-1} with a N.P.L./Grubb-Parsons Michelson type interferometer with a Golay detector; ○, MBBA (nematic) at 296 ± 0.5 K at 2 cm^{-1} resolution, taken with a Beckman lamellar grating interferometer with a helium cooled Putley detector at the N.P.L., Teddington. Path length difference = 0.77 mm with polypropylene windows in a R.I.I.C. VC-01 cell; □, microwave measurement.¹¹

MBBA molecules will be of the order of magnitude dictated by the interactions of their component phenyl rings, i.e. we neglect the presence of the substituent groups of the p, p' positions, and treat the barrier as due merely to the phenyl rings.

Barrier heights were calculated from the difference between the net energy (dispersion and repulsion) of the group of seven benzene molecules in the idealised configuration of minimum energy (fig. 6(a)) and the net energy of the group in other configurations (fig. 6(b) and 6(c) which might be taken to represent plausible energy profiles as the central molecule rotates (i) with the surrounding molecules fixed and (ii) with the surrounding molecules taking part in the process. Clearly since the model is a static one, the profiles of fig. 6(b) and fig. 6(c) can represent only two situations out of many possible simulations of the barrier to rotation of the central molecule.

The difference in the net energies is then doubled to give the barrier height (since MBBA has two phenyl rings). The details of the calculation are exactly as explained by Rae and Mason for solid benzene, except that here, only nearest neighbour interactions are considered. These calculations can at best achieve an order of magnitude validity as only some particular configurations are evaluated, including specifically two instances which are possible extremes, representing reasonable maximum and minimum values of the barrier.

First, the molecules, seen in section perpendicular to their aligned lengths, are lying parallel (fig. 6(a)). The net energy (relative to the vapour state) for this (idealised) configuration was found to be 67 kJ mol^{-1} , taking account of the two sets of seven benzene rings representing the MBBA molecules. If the rotation of the central molecule is now attempted, keeping the six nearest neighbours fixed, then the system experiences an unrealistic net repulsion of $+152 \text{ kJ mol}^{-1}$ after the central molecule has rotated 44° . This is overwhelmingly due to the closest approaching hydrogens on neighbouring rings, whose van der Waals radii overlap in this position. This unlikely configuration for the rotation also produces calculated energy profiles which have narrow barriers and broad wells (compared to the $V = f(\sin^2 \theta)$ function used in the Brot and Wyllie models), whereas the Brot model predicts broad barriers and narrow wells.

However, all the molecules of the nematic phase will have enough thermal energy to allow for the cooperative participation of the nearest neighbours resulting in the central molecule rotating against a smaller barrier than in this extreme case. To approximate an extreme participative mechanism (i.e. minimum barrier), the configurations of fig. 6(c) are used. It is found in this case that the net energy in the well is -65 kJ mol^{-1} and is -56 kJ mol^{-1} at the barrier, giving the height of 9 kJ mol^{-1} . The energy profile in this case is made up of a broad barrier and a narrow well, in qualitative (if not quantitative) agreement with the Brot prediction.

The grant of a Dr. Samuel Williams studentship from University College, Aberystwyth, is acknowledged by M. W. E. and the assistance provided at the N.P.L., Division of Electrical Sciences.

- ¹ Mansel Davies, G. W. F. Pardoe, John Chamberlain and H. A. Gebbie, *Trans. Faraday Soc.*, 1970, **66**, 273.
- ² G. W. F. Pardoe, *Spectrochim. Acta A*, 1971, **27**, 203.
- ³ M. Davies, G. W. F. Pardoe, J. E. Chamberlain and H. A. Gebbie, *Trans. Faraday Soc.*, 1968, **64**, 847.
- ⁴ N. E. Hill, *J. Phys. A*, 1969, **2**, 398.
- ⁵ N. E. Hill, *Chem. Phys. Letters*, 1968, **2**, 5.
- ⁶ Mansel Davies, *Ann. Rep. Chem. Soc. A*, 1970, **67**, 67.
- ⁷ A. I. Baise, *Chem. Phys. Letters*, 1971, **9**, 627.
- ⁸ I. Darmon, A. Gerschel and C. Brot, *Chem. Phys. Letters*, 1970, **7**, 53.
- ⁹ I. Darmon, A. Gerschel and C. Brot, *Chem. Phys. Letters*, 1971, **8**, 454.
- ¹⁰ I. Larkin, to be published; R. Haffmans and I. W. Larkin, *J.C.S. Faraday II*, 1972, **68**, 1729.
- ¹¹ P. Maurel and A. H. Price, personal communication.
- ¹² H. A. Gebbie and R. Q. Twiss, *Rep. Progr. Phys.*, 1966, **46**, 396.
- ¹³ A. I. Baise, *Thesis* (Univ. of Wales, 1971).
- ¹⁴ A. de Vries, *Mol. Cryst. Liquid Cryst.*, 1970, **11**(4), 361.
- ¹⁵ G. W. F. Pardoe, *Thesis* (Univ. of Wales, 1969).
- ¹⁶ N. E. Hill, W. E. Vaughan, A. H. Price and M. Davies, *Dielectric Properties and Molecular Behaviour* (van Nostrand-Reinhold, London, 1969), chap. 1, 2.
- ¹⁷ M. E. van Krefeld, R. M. van Aalst and J. van der Elksen, *Chem. Phys. Letters*, 1970, **4**, 580.
- ¹⁸ G. W. F. Pardoe, *Trans. Faraday Soc.*, 1970, **66**, 2699.
- ¹⁹ S. R. Polo and M. K. Wilson, *J. Chem. Phys.*, 1955, **23**, 2376.
- ²⁰ C. Brot, *J. Physique*, 1967, **28**, 789.
- ²¹ B. Lassier and C. Brot, *Chem. Phys. Letters*, 1968, **1**, 581.
- ²² Ivan Haller, H. A. Huggins and M. J. Freiser, *Mol. Cryst. Liquid Cryst.*, 1972, **16**, 53.
- ²³ J. O. Hirschfelder, *J. Chem. Phys.*, 1940, **8**, 431.
- ²⁴ N. E. Hill, *Proc. Phys. Soc.*, 1963, **82**, 723.
- ²⁵ G. Wyllie, *J. Phys. Chem.*, 1971, **4**, 564.
- ²⁶ A. I. M. Rae and R. Mason, *Proc. Roy. Soc. A*, 1968, **304**, 487.
- ²⁷ G. Maier and A. Saupe, *Mol. Cryst. Liquid Cryst.*, 1966, **1**, 515.